06

Plasmonic gold and silver nanoparticles for creating biointerfaces

© U.E. Kurilova,[1,2] D.V. Novikov,[3] Yu.V. Chumachenko,[3] A.M. Tarasov,[3] S.V. Dubkov,[3] D.G. Gromov,[3] I.A. Suetina,[4] L.I. Russu,[4] M.V. Mezentseva,[4] A.Yu. Gerasimenko[1,2]

[1] Institute for Bionic Technologies and Engineering, Sechenov First Moscow State Medical University, Sechenov University, 119991 Moscow, Russia
[2] Institute of Biomedical Systems, National Research University of Electronic Technology, „MIET“, 124498 Moscow, Zelenograd, Russia
[3] Institute of perspective materials and technologies, National Research University „MIET“, 124498 Moscow, Zelenograd, Russia
[4] N.F. Gamaleya National Research Centre for Epidemiology and Microbiology. of the Ministry of Health of the Russian Federation, 123098 Moscow, Russia
e-mail: kurilova_10@mail.ru

Received December 19, 2025
Revised December 19, 2025
Accepted December 19, 2025

This paper presents the results of studying gold and silver nanoparticle arrays immobilized on a silicon substrate to explore the potential of using them to create optically activated biointerfaces. The nanoparticles were formed using vacuum thermal evaporation and rapid thermal annealing. Varying the initial film thickness from 5 to 100 nm and the annealing temperature allowed us to obtain nanoparticle arrays with different morphologies. Quantitative parameters of the cellular response were studied, including the number of cells, the total area occupied by cells, and the average size of an individual cell, as well as the cell distribution and morphology on the surface of the nanoparticle substrate after incubation for 48 hours. The highest cellular activity was observed on gold nanoparticles obtained from 5 and 10 nm films, as well as on silver nanoparticles with a film of 5 nm. Thus, the studied nanoparticle arrays have potential for use in creating interfaces for stimulating cells and tissues.

Keywords: plasmon resonance, vacuum thermal evaporation, rapid thermal annealing, biocompatibility, stimulation.

DOI: 10.61011/TP.2026.05.63519.330-25

Introduction

Socially sensitive diseases and damage to the central and peripheral nervous system caused by degenerative processes (Alzheimer disease, Parkinson disease), the consequences of strokes or mechanical injuries, are among the most complex problems in today's medicine and are the main causes of irreversible functional disorders and long-term disability of patients [1]. The recovery from such damage is a serious problem because of sophisticated physiology and limited regenerative capacity of tissue due to complexity of its architectonics and the presence of inhibitory factors in the tissue microenvironment [2]. In addition, neuropathic pain resulting from spinal cord injuries, peripheral nerves, or degenerative diseases is often resistant to traditional pharmacotherapy and often requires new neuromodulation strategies to be used [3].

In terms of maintaining the vital activity of cells and tissues, including nervous ones, one of the promising areas of support is creation of biointerfaces based on tissue engineering approaches that envisages development of an artificial structure with its composition and properties contributing to the improved cell growth and formation of a healthy tissue [4]. It is known that for better cell proliferation on artificial tissue engineering structures, it is preferable to use growth factors and various types of stimulation, the most common of which are mechanical, electrical or optical ones [5]. The new generation biointerfaces with a specially selected surface structure are not only capable of mechanical support of the axons growth and neurons survival, but also purposefully stimulate their functional activity and, among other things, can be used to suppress pain signals [6].

The advantages of the optical method include high spatial and temporal precision, absence of contact between the stimulating device and the tissue, as well as potential compatibility with neuroimaging methods. However, the direct application of laser radiation to activate neurons requires either genetic modification of cells (optogenetics) or the use of high power, which can cause photothermal damage [7]. In this regard, nanoplasmonic technologies that allow local conversion of light into biocompatible physical signals are attracting a growing attention.

Metal nanoparticles, which have unique optical properties associated with localized surface plasmon resonance [8], have a pivotal role in such systems. In metals, surface electrons behave like free charges that can be excited by an electromagnetic wave. Thus, plasmon waves arise both from mechanical vibrations of the charge and from electromagnetic vibrations of the electric field [9]. If this phenomenon occurs at the nanometer scale, it is

the result of the limitation of the electric field inside a small metal particle. When these nanoparticles interact with light, an oscillating electric field causes electrons to oscillate at the same frequency as an electromagnetic wave, which is consistent with their plasmonic electron cloud and its distribution throughout the volume of the nanoparticle. These nanoparticles are able to effectively absorb light in a certain wavelength range (including in the near infrared, in which the biological tissue is most transparent due to the intersection of the areas of least absorption of radiation by water and blood hemoglobin), converting it into heat. In tissue engineering, plasmonic nanoparticles are used to stimulate cells on scaffolds due to their ability to amplify electromagnetic fields and locally increase temperature under the influence of laser radiation. This phenomenon causes such an effect as increased cellular metabolism and proliferation because of moderate thermal and optical stimulation, which activates the biochemical signaling pathways. The possibility of local and controlled heating within a scaffold free from any lesion of the surrounding tissues provides conditions for the targeted stimulation of cell growth and improved tissue regeneration. By varying the power and irradiated area of the scaffold, it becomes possible to control cell growth.

Among plasmonic nanoparticles, a special place is given to gold and silver nanoparticles. The gold nanoparticles in biomedicine may be used in a slew of applications — they are used in genomics, biosensorics, enzyme immunoassay, clinical chemistry, as well as in methods of detection and photothermolysis of pathogenic microorganisms and tumor cells [11,12]. In addition, they are actively used for the targeted delivery of therapeutic agents — including drugs, peptides, DNA and antigens — and in optical bioimaging, including monitoring of cellular and tissue structures using advanced nanophotonic recording systems [13,14]. Silver nanoparticles are widely used for wound treatment, in coatings of surgical instruments, bone implants, in biosensorics and nanoelectronics [15,16]. Silver nanoparticles also demonstrate high efficacy against a wide range of pathogenic microorganisms. According to numerous studies, both gold and silver nanoparticles have high biocompatibility [17–22].

Thus, the use of gold and silver nanoparticles in combination with laser or optical stimulation on tissue-engineered scaffolds represents a promising approach to increasing the proliferative potential of cells and improving the regenerative properties of tissues through effective stimulation at the nanoscale.

It is crucial to allow for the concentration and size of nanoparticles, since high concentrations or inappropriate sizes can cause cytotoxicity, damage to the cytoskeleton, and inhibition of proliferation. Optimal functionalization and dosage of plasmonic nanoparticles ensure their biocompatibility and stimulating effect. The surface charge of gold and silver nanoparticles is neutralized by an undesirable effect of aggregation. The use of plasmonic nanoparticles deposited on a substrate avoids undesirable aggregation, and by limiting mobility in the culture medium opens up opportunities for a high-precision external controlled exposure. Laser radiation can be used for a selective activation of nanostructures in order to change the cells behavior in the desired way and, thus, provide a selective activation of the tissue structures.

This paper outlines a comprehensive study of samples of plasmonic gold and silver nanoparticles arrays obtained by vacuum thermal evaporation (VTE) and rapid thermal annealing (RTA). The surface structure of the samples was studied by scanning electron microscopy (SEM). A comprehensive assessment of cell growth during incubation with samples was carried out, including the number of cells, occupied area and morphology, using quantitative analysis and fluorescence microscopy. The most promising samples in terms of optically activated neural interfaces for noninvasive modulation of nerve cell activity have been selected.

1. Materials and methods of research

Silicon wafers 1 by 1 cm in size with a thermal oxide layer of 300 nm were used as substrates.

1.1. Formation of silver nanoparticle arrays

To form nanoparticle arrays on the substrates, silver samples 3, 6, 9, 30, and 60 mg were evaporated by VTE method to obtain films with virtual thicknesses of 5, 10, 15, 50, and 100 nm, respectively. The current was about 7 A at 220 V phase voltage, which approximately corresponded to 1.6 kW of power supplied to the evaporator. Evaporation was performed at a distance of 20 cm between the molybdenum boat-evaporator and the substrates and a residual atmosphere of 10^{-5} Torr until complete evaporation of the suspension, ~ 60 s, the substrate holder was fixed rigidly above the evaporator, the installation scheme is similar to that presented in [23]. To obtain arrays of plasmonic nanoparticles from the formed films, substrates with a deposited silver layer were annealed by RTA method in a vacuum of 10^{-5} Torr. The samples were exposed for 10 s at a temperature of 250 °C for 5 nm, 400 °C for 10 and 15 nm, 670 °C for 50 nm and 750 °C for 100 nm.

1.2. Formation of gold nanoparticles array

To form arrays of gold nanoparticles on the substrates, the 7.5, 15, 22.5, 75, and 150 mg samples were vaporized by VTE method to obtain films with virtual thicknesses of 5, 10, 15, 50, and 100 nm, respectively. The current was about 7 A at 220 V phase voltage, which approximately corresponded to 1.6kW of power supplied to the evaporator. Evaporation was performed at a distance of 20 cm between the molybdenum boat-evaporator and the substrates and a residual atmosphere of 10^{-5} Torr until the suspension was completely evaporated, ~ 60 s. To obtain arrays of plasmonic nanoparticles from the formed films, substrates

with a deposited layer of gold were annealed by BTO method in a vacuum of 10^{-5} Torr. The samples were annealed for 10 s at a temperature of 500 °C for 5, 10 and 15 nm, 760 °C for 50 nm and 860 °C for 100 nm.

2. Studies by SEM method

During the samples formation, a satellite sample was prepared for each of them to control the material obtained in these conditions. The satellite samples were studied using a scanning electron microscope FEI Helios NanoLab 650 (FEI Ltd., Hillsboro, OR, USA). The measurements were made at an accelerating electron beam voltage of 5 kV, the electron probe current — 86 pA, and the pressure in the vacuum chamber was $1.6 \cdot 10^{-4}$ Pa. Based on SEM images the sizes of nanoparticles were calculated using „Image J“ software.

2.1. Studies of cellular growth on samples

For *in vitro* studies, a fibroblast cell line from N.F. Gamalei National Research Center for Epidemiology and Microbiology was used. The samples were placed on the bottom of wells of a 12-well culture plate, then a suspension of cells in a seeding concentration of $4.9 \cdot 10^5$ cell/ml was added to each sample. The sample plates were kept in CO_2 thermostat for 48 hours after the cells were planted. At the end of incubation, the cells on the samples were stained with Hoechst 33342 dye and viewed on Olympus IX73 fluorescence microscope. Five microscopic images were obtained for each sample. The number of cells on each of the samples was found using „Image J“ software.

3. Results and discussion

3.1. Characterization of the fabricated samples

For arrays of gold and silver nanoparticles formed by vacuum-thermal evaporation followed by rapid thermal annealing, SEM studies were carried out (Fig. 1). This method allows obtaining three-dimensional images of the surface with high resolution and a large depth of field, which provides a detailed study of the morphology of nanoparticles and their distribution.

Nanoparticles were formed as a result of disintegration of continuous metal films during high-temperature annealing, in which the system tends to minimize surface and interfacial energies. Varying the virtual thickness and annealing parameters allowed to obtain the arrays of gold and silver nanoparticles with different morphologies — from isolated nanoparticles to interconnected percolation networks. Arrays of isolated nanoparticles are of the greatest interest in this study, since for the purpose of developing neurostimulating coatings, a localized controlled effect on the cells is required, which is realized in the presence of discrete plasmonic nanostructures themselves [8]. Although connected networks have interesting conductive or optical properties, they do not provide the necessary spatial selectivity and can interfere with cell adhesion, making them less suitable to get the required result.

Gold nanoparticles were represented by separate elements for 5 and 10 nm virtual film thicknesses (annealing temperature 500 °C), while in the case of a 10 nm film, a smaller particle size and shape was observed, the average size was 54 nm and the shape was close to rounded. The nanoparticles obtained from films with a virtual thickness of 5 nm had an average size of 59 nm and a flatter shape. The share of the covered area was 46 % and 36 % for nanoparticles from films with a virtual thickness of 5 and 10 nm, respectively. Despite the large initial thickness, the particles from the film with a virtual thickness of 10 nm showed a smaller variation in size and shape, which may indicate more complete coalescence at the same annealing temperature.

Thus, a nonmonotonic dependence was observed for gold nanoparticles. During transition from a virtual thickness of 5 to 10 nm, the average particle diameter decreased slightly from 59 to 54 nm, while the surface density increased. This observation can be explained by the fact that at 500 °C and a larger amount of material (10 nm), either more complete coalescence is observed at the same annealing temperature, or the film restructuring process results not in the growth of existing particles, but in the formation of more new nuclei having a smaller average size. At large virtual film thicknesses, the nanoparticles formed a connected array with an average nanosheet cross-section of 53 nm, the area coverage was 48 % for nanoparticles with a virtual film thickness of 15 nm. When the annealing temperature grew up to 760 °C and 860 °C a connected percolation network was observed with a sharp increase in the coating fraction for the film thicknesses of 50 and 100 nm. At large virtual film thicknesses, the nanoparticles formed a connected array, the area coverage was 48 % for nanoparticles with a virtual film thickness of 100 nm, for a 50 nm film the remaining material was 84 %.

In case of silver nanoparticles, the size of individual particles correlated with the virtual thickness of the film. This may be due to both the lower melting point of silver (961 °C) compared to gold (1064 °C) [24,25] and the lower surface tension energy, which provides increased mobility of silver atoms on the substrate during annealing [26]. For samples with a virtual coating thickness of 5 nm, individual particles with an average size of 17 nm were observed, for a virtual thickness of 10 nm, the average particle size was 38 nm, the surface coverage was 28 % and 32 %, respectively. The virtual film thickness of 15 nm corresponded to the average sample size of 48 nm, the nanoparticles covered 25 % of the surface. The surface area occupied by the nanoparticles remained relatively constant, which may indicate a mechanism of growth mainly due to the increase in existing particles rather than the formation of new ones. With higher virtual thickness of the film, it deforms without disintegrating into individual nanoparticles,

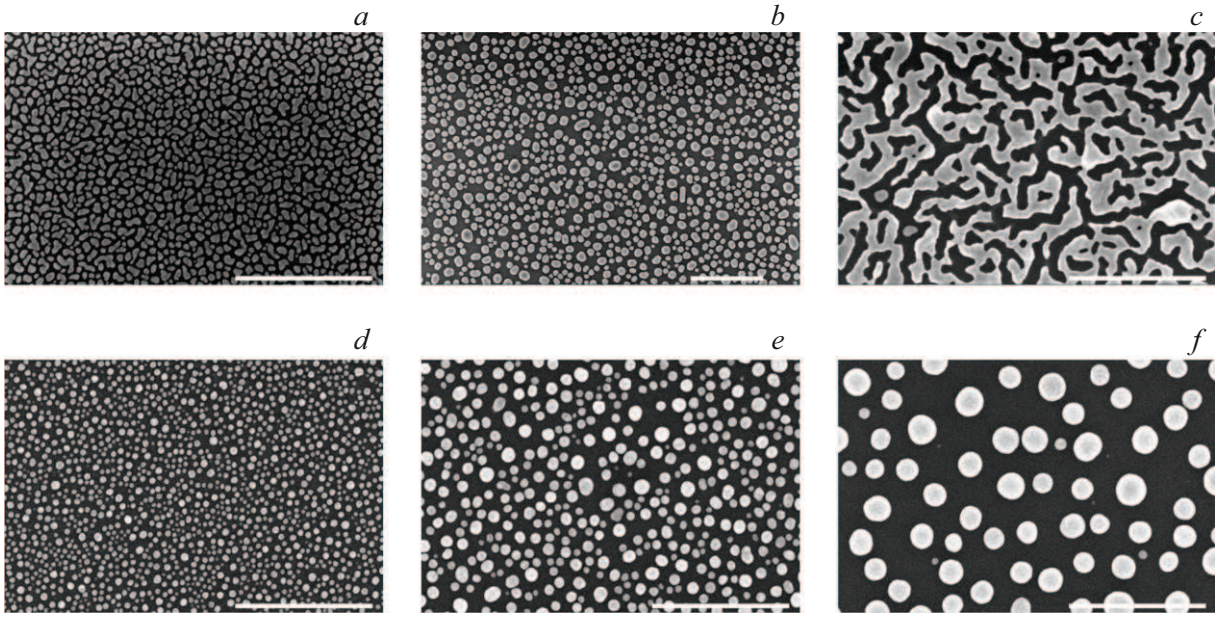

Figure 1. SEM-images of the gold nanoparticles arrays (*a*–*c*) and silver nanoparticles arrays (*d*–*f*). Virtual thickness of films — 5 (*a, c*), 10 (*b, d*) and 15 nm (*c,f*). Scale line — 500 nm.

which goes beyond the morphological regime, which is of primary interest for this study of arrays of isolated nanoparticles.

The obtained morphological characteristics are crucial for subsequent biological tests. Separate, well-isolated nanoparticles (gold and silver samples with virtual thicknesses of 5 and 10 nm) are preferable from the biocompatibility standpoint, since they are less likely to cause mechanical stress in the cell membrane and provide a more uniform distribution of the stimulating factor (for example, a local electric field). The nanoparticle sizes (15–60 nm) and their distribution density (25 %–50 % coating) in samples with thickness of 5–15 nm correspond to the range at which biocompatibility is maximized and effective optical activation is possible due to local plasmon resonance. Denser structures can limit cell adhesion and migration, while too sparse arrays do not provide sufficient stimulating signal.

3.2. Cell growth studies on formed samples

To estimate the biocompatibility and potential use of the fabricated samples as substrates for optical stimulation, three quantitative parameters of fibroblast behavior were analyzed: the absolute number of cells, the total area occupied by cells, which reflects the degree of adhesion and spreading, as well as the average size of an individual cell, correlating with morphological maturity and the full performance of its functions by the cell. Isolated gold and silver nanoparticles (virtual thickness 5, 10, 15 nm) were of the greatest interest; samples with a larger virtual thickness characterized by the formation of continuous conductive layers were included in biological tests as a reference group to estimate the impact of high coating density on behavior of cells. All samples were compared with the control sample — a smooth silicon substrate without nanoparticles. Based on the obtained data the graphs were plotted (see Fig. 2).

The results showed that all the studied nanostructured surfaces, both gold and silver, contributed to a better cell adhesion to the materials and higher fibroblast spreading compared with the control substrate. This was indicated by a higher cell density and size for all samples compared to the control sample, which was quite benign for subsequent proliferation and formation of a cellular monolayer. Enhanced adhesion, possible due to suitable surface properties, is an extremely important prerequisite for the subsequent proliferation, migration and formation of a stable cellular monolayer, especially given that such systems will further be used in tissue engineering and neuromodulation.

According to the findings, the largest number of cells is found on samples with silver particles with a virtual film thickness of 50 and 5 nm. The maximum number of cells in gold nanoparticles was obtained for samples with virtual thicknesses of 5 and 10 nm. At the same time, the area occupied by the cells in case of gold particles exceeds this indicator of silver particles for all the considered sizes, except 5 nm, the largest cell coverage is observed for 10, 5 and 15 nm samples. The cell size for gold nanoparticles also exceeds, on average, the cell size on silver nanoparticles and is the maximum for samples with a virtual film thickness of 15, 10, and 5 nm.

Gold nanoparticles were featuring a consistent and predictable bioactivity pattern: the highest cell number, area occupied, and average cell size were observed in samples with virtual film thicknesses of 5 and 10 nm (corresponding to average particle sizes of 59 and 54 nm and a surface

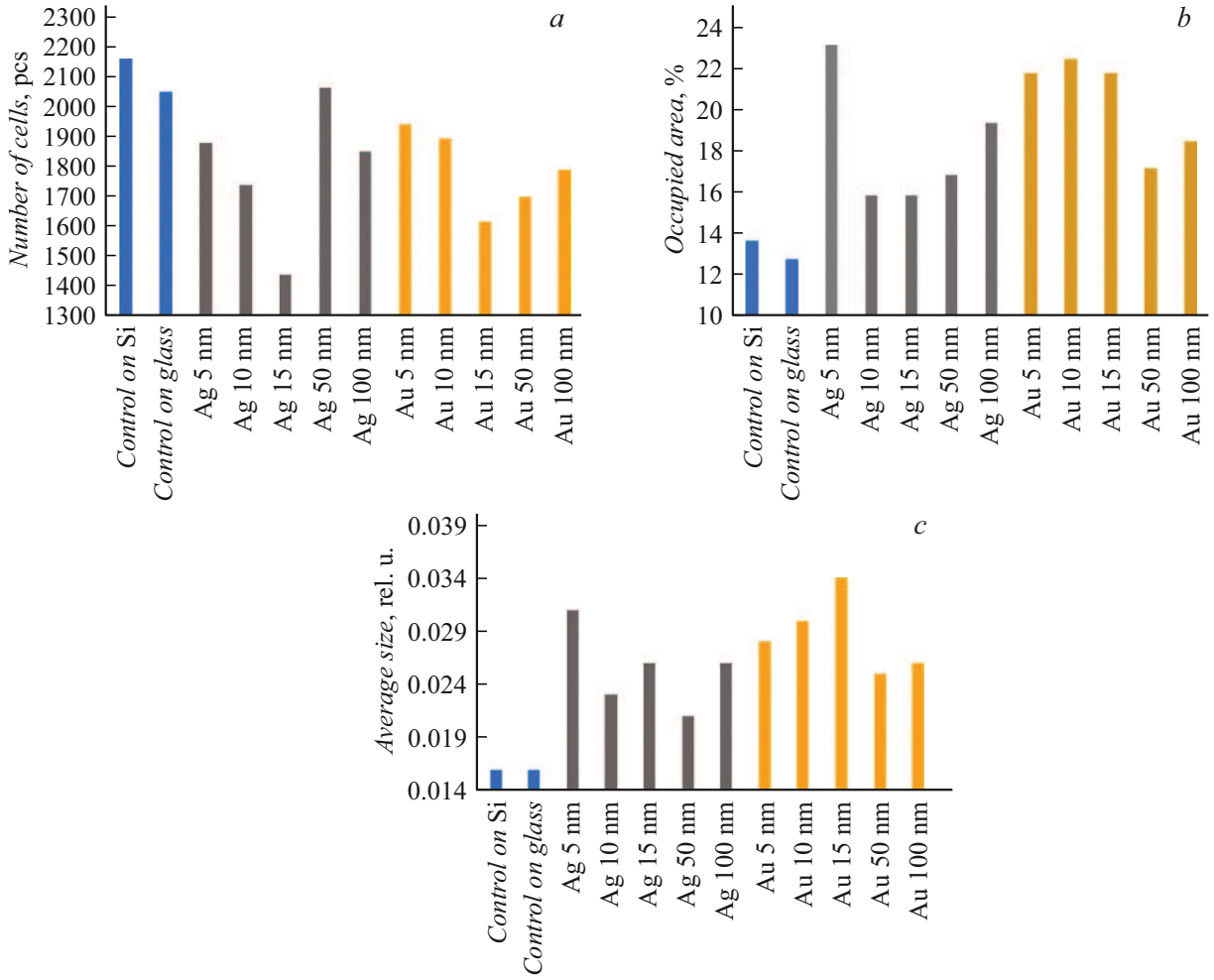

Figure 2. Results of calculating cellular activity on nanoparticle samples: *a* — total number of cells, *b* — area occupied by cells, *c* — cell size.

coverage of 36 %–46 %). This morphology provides the best nano-topography — it is quite dense to accommodate a multiplicity of the contact points, but not continuous so as not to limit the membrane mobility [27]. It should be underscored that the area occupied by cells on substrates with golden particles arrays exceeded that for all samples with silver nanoparticles, except for those obtained from films with a virtual thickness of 5 nm, which further emphasizes the biocompatibility of gold in the studied range. Given the obtained data, nanoparticles from the films with virtual thicknesses of 5 and 10 nm are the most promising for further experiments in case of gold.

In case of silver particles, despite the fact that the largest number of cells was detected on a sample with a virtual film thickness of 50 nm, the occupied area and average size for this sample were the smallest, therefore, it may be somewhat complicated to grow a homogeneous layer of cells on the required surface later. Such a discrepancy may indicate that the cells on this surface remain in a rounded shape with insufficient adhesion, presumably caused by excessive density of nanostructures or the potential cytotoxic effect of silver ions during prolonged cultivation. This condition does not contribute to formation of a stable monolayer and can lead to cell detachment in dynamic conditions, which makes this sample less suitable for practical use. A sample with silver particles obtained from a 5 nm virtual thickness film demonstrates the best results in terms of the coating area and cell size with a sufficient total number of cells. This result is similar to that for the gold nanoparticle samples, thus making such silver nanoparticle arrays as potentially suitable for further study, especially given the antimicrobial properties of silver, which may be useful in preventing the implantation induced infectious complications [28].

Figure 3 shows microscopic images of fibroblasts on the surface of samples. Morphological analysis of cells performed using fluorescence microscopy after staining of Hoechst 33342 nuclei proved high biocompatibility of the studied nanoparticle arrays. On all samples, the cell nuclei retained a normal rounded or oval shape, uniform fluorescence, and no signs of chromatin condensation or fragmentation, which excludes any manifestations of apop-

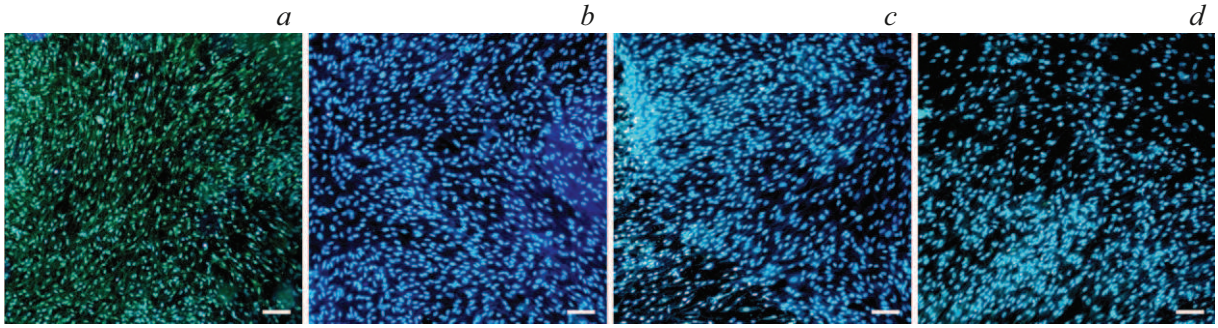

Figure 3. Fluorescent micrographs of fibroblasts after 48 h, cultivation on various substrates: *a* — control (smooth silicon substrate); *b* — gold nanoparticles (virtual film thickness 5 nm); *c* — gold nanoparticles (virtual film thickness 10 nm); *d* — silver nanoparticles (virtual film thickness 5 nm). All images had the same magnification, scale line — 100 μm.

tosis or acute toxic effects [29]. One or two slightly colored rounded inclusions (nucleoli) surrounded by a uniformly fluorescent nuclear mass were visualized in the fibroblast nuclei, which corresponded to the normal structure of the metabolically active cells.

The cells on most of the substrates showed a characteristic elongated (fusiform) shape, indicating adhesion and active spreading. This is especially visible on substrates with gold nanoparticles obtained from films with virtual thicknesses of 5 and 10 nm, where cells formed oriented, elongated shapes with a uniform distribution of nuclei along the cytoplasm — a sign of mature, functionally active fibroblast [30].

On silver nanoparticles from films with a virtual thickness of 5 nm, the cell morphology also did not differ from that on the control sample, although the degree of spreading in some areas was somewhat less pronounced, which is consistent with the percentage of the occupied area. At the same time, on silver nanoparticles from films with a virtual thickness of 50 nm, despite the presence of nuclei, cells more often retained a more compact, slightly stretched shape, which visually confirms limited adhesion and decreased functional activity, despite the high number of cells in total.

Thus, fluorescence imaging not only proves the absence of any cytotoxicity of all the studied materials but also provides a qualitative estimate of the cells adhesion and spreading level. The combination of quantitative and morphological data enables to identify gold nanoparticles obtained from films with a virtual thickness of 5 and 10 nm, and silver nanoparticles from films with a virtual thickness of 5 nm as the most promising candidates for the development of biointerfaces designed for optical stimulation and support in regeneration of damaged tissues, including the nervous system.

The resulting improvement in cell adhesion and spreading in the absence of optical irradiation for these samples is primarily due to topographic stimulation. It is known that nanostructured surfaces with a certain element size and roughness can enhance cell adhesion by increasing the contact area and modulating the formation of focal adhesions [31,32]. Here, the arrays of isolated gold and silver nanoparticles create just such a biomimetic surface. The observed improvement in cells growth leads to the occurrence of an optimal cellular monolayer for subsequent effective plasmon stimulation, which will be realized under laser irradiation due to local amplification of the electromagnetic field and moderate photothermal effect [33–36].

Differences in cells response to gold and silver nanoparticles of the same size may be associated not only with topography, but also with surface chemistry. Gold is chemically inert and does not release significant amounts of ions in physiological conditions, whereas silver, even in the form of immobile structures, can gradually oxidize to form Ag^+ ions having a pro-oxidant effect [37]. Silver at low concentrations may not cause acute cytotoxicity, however, a decrease in growth dynamics is possible, which is observed as a lowering of spreading area and average cell size, especially in dense arrays.

For the fibroblast cells, larger area and elongated morphology are directly related to their synthetic activity: large, spreaded cells more actively release extracellular matrix components (collagen, fibronectin) and participate in the tissue regeneration. Thus, larger average cell size on substrates with arrays of gold nanoparticles may indicate not only good adhesion, but also an increased regenerative potential of such surfaces. Moreover, the optimal nanotopography revealed for gold particles obtained from the films with a virtual thickness of 5–10 nm coincided with the range where maximum amplification of the local electromagnetic field was provided during laser irradiation, which opens the way to non-invasive optical stimulation of cellular activity in further experiments.

Conclusion

This paper outlines the findings of comprehensive studies of cell growth in arrays of plasmonic gold and silver nanoparticles formed by methods of vacuum thermal evaporation and subsequent rapid thermal annealing. It has been

demonstrated that the morphology of the obtained arrays can be precisely controlled by varying the virtual thickness of the initial film and the annealing temperature.

It has been experimentally proved that the synthesized nanoparticles enhance the adhesion and proliferation of the fibroblast cells. Gold nanoparticles of 5 and 10 nm in size and silver nanoparticles of 5 nm demonstrated the highest efficiency. The gold nanoparticles arrays showed maximum number of cells, maximal occupied area and average size, as well as a characteristic elongated morphology indicating the normal process of cell growth. The size and shape of the nanoparticles corresponded to the range at which the maximum amplification of the local electromagnetic field is realized due to localized surface plasmon resonance in the visible and near infrared ranges. Among silver nanoparticles, the best results were observed for the nanoparticles obtained from 5 nm thick films, which was comparable to optimal gold samples in terms of cell adhesion and morphology. Though silver is prone to the ion release, the coating density and the size of the nanoparticles are small enough to exhibit this effect. In this case, in addition to biocompatibility, it opens up the possibility of using the antimicrobial properties of silver, which is extremely important for implantable devices.

Thus, the obtained nanoparticles simultaneously meet the biological requirements (adhesion, spreading, lack of toxicity) and physical criteria (the possibility of stimulation by optical radiation). Gold nanoparticles obtained from 5 and 10 nm thick films and silver nanoparticles from 5 nm thick films have been identified as the most promising candidates for further research of interfaces for optical stimulation and regeneration of damaged tissues, in particular, the nervous system. The resulting nanoparticles can be used both unchanged and embedded in other materials, making it possible to take advantage of combined systems and conduct targeted stimulation. When irradiated with a laser in the resonant range, nanoparticles contribute to the activation of ion channels in the cell membrane, which can be used both to stimulate regeneration and to suppress the pathological generation of pain impulses. Unlike traditional electrical implants, such systems do not require wires, power supplies, or complex microelectronics, which simplifies their design, reduces the risk of an inflammatory reaction, and increases durability.

The study was performed using the equipment of the Core Shared Research Facility (CSRF) „Center of laser technologies in medicine“.

Funding

This study was performed as part of a large research project and funded by the Russian Federation represented by the Ministry of Science and Higher Education of the Russian Federation under Agreement № 075-15-2024-555 of April 25, 2024.

Conflict of interest

The authors declare that they have no conflict of interest.

References

[1] R. Boni, A. Ali, A. Shavandi, A.N. Clarkson. J. Biomed. Sci., **25** (1), 90 (2018). DOI: 10.1186/s12929-018-0491-8
[2] Y.-S. Borghei, S. Hosseinkhani, M.R. Ganjali. J. Adv. Res., **39**, 61 (2022). DOI: 10.1016/j.jare.2021.11.006
[3] S. Cherevko, C.-H. Chung. Electrochem. Commun., **13** (1), 16 (2011). DOI: 10.1016/j.elecom.2010.11.001
[4] G.P. Chuy, B.P. Savi, C.P. Pavi, G.A. Filipe, D. Robl, G. Fongaro, W.L. da Silva, F.A. Ferreira. Bio Nano Sci., **15** (3), 380 (2025). DOI: 10.1007/s12668-025-02005-2
[5] L. Colloca, T. Ludman, D. Bouhassira, R. Baron, A.H. Dickenson, D. Yarnitsky, R. Freeman, A. Truini, N. Attal, N.B. Finnerup, Ch. Eccleston, E. Kalso, D.L. Bennett, R.H. Dworkin, S.N. Raja. Nat. Rev. Dis. Primers, **3** (1), 17002 (2017). DOI: 10.1038/nrdp.2017.2
[6] M.J. Dalby, N. Gadegaard, R. Tare, A. Andar, M.O. Riehle, P. Herzyk, Ch.D.W. Wilkinson, R.O.C. Oreffo. Nat. Mater., **6** (12), 997 (2007). DOI: 10.1038/nmat2013
[7] L.R. Doblado, C. Martínez-Ramos, M.M. Pradas. Front. Nanotechnol., **3**, 643507 (2021). DOI: 10.3389/fnano.2021.643507
[8] I. Egry, E. Ricci, R. Novakovic, S. Ozawa. Adv. Colloid Interface Sci., **159** (2), 198 (2010). DOI: 10.1016/j.cis.2010.06.009
[9] Z. Fekete, Á.C. Horváth, A. Zátonyi. J. Neural Eng., **17** (5), 051003 (2020). DOI: 10.1088/1741-2552/abb3b2
[10] W. Huang, V. Rajendran, M. Chan, M. Hsiao, H. Chang, R. Liu. Adv. Opt. Mater., **11** (11), 2202061 (2023). DOI: 10.1002/adom.202202061
[11] I. Ielo, G. Rando, F. Giacobello, S. Sfameni, A. Castellano, M. Galletta, D. Drommi, G. Rosace, M. R. Plutino. Molecules, **26** (19), 5823 (2021). DOI: 10.3390/molecules26195823
[12] L. Dykman, N. Khlebtsov. Chem. Soc. Rev., **41**, 2256 (2012). DOI: 10.1039/c1cs15166e
[13] S. Siddique, J.C.L. Chow. Appl. Sci., **10** (11), 3824 (2020). DOI: 10.3390/app10113824
[14] P. Si, N. Razmi, O. Nur, S. Solanki, C.M. Pandey, R.K. Gupta, B.D. Malhotra, M. Willander, A. de la Zerda. Nanoscale Adv., **3**, 2679 (2021). DOI: 10.1039/D0NA00961J
[15] A.-C. Burduşel, O. Gherasim, A.M. Grumezescu, L. Mogoantă, A. Ficai, E. Andronescu. Nanomaterials, **8** (9), 681 (2018). DOI: 10.3390/nano8090681
[16] S.S.D. Kumar, N.K. Rajendran, N.N. Houreld, H. Abrahamse. Int. J. Biol. Macromol., **115**, 165 (2018). DOI: 10.1016/j.ijbiomac.2018.04.003
[17] D. Mahl, J. Diendorf, S. Ristig, C. Greulich, Z.-A. Li, M. Farle, M. Köller, M. Epple. J. Nanoparticle Res., **14** (10), 1153 (2012). DOI: 10.1007/s11051-012-1153-5
[18] J.R. Kadhim, E.H. Karsh, Z.J. Taqi, M.S. Jabir. Mater. Today: Proc., **42** (5), 3041 (2021). DOI: 10.1016/j.matpr.2020.12.826
[19] N.R.S. Sibuyi, K.L. Moabelo, A.O. Fadaka, S. Meyer, M.O. Onani, A.M. Madiehe, M. Meyer. Nanoscale Res. Lett., **16**, 174 (2021). DOI: 10.1186/s11671-021-03632-w
[20] A.H. Hashem, A.M. Shehabeldine, O.M. Ali, S.S. Salem. Polymers, **14** (11), 2293 (2022). DOI: 10.3390/polym14112293

[21] D.S. Ipe, P.T.S. Kumar, R.M. Love, S.M. Hamlet. Front. Microbiol., **11**, 1074 (2020). DOI: 10.3389/fmicb.2020.01074
[22] J. Zhang, L. Mou, X. Jiang. Chem. Sci., **11**, 923 (2020). DOI: 10.1039/C9SC06497D
[23] A.M. Tarasov, D.V. Novikov, D.V. Gorelov, S.S. Generalov, V.V. Amelichev. Fotonika, **17**, (6), 488 (2023) (in Russian). DOI: 10.22184/1993-7296.FRos.2023.17.6.488.496
[24] Y. Huang, X. Lü, R. Chen, Y. Chen. Regen. Biomater., **7** (2), 221 (2020). DOI: 10.1093/rb/rbz051
[25] V.S. LeBleu, E.G. Neilson. FASEB J., **34** (3), 3519 (2020). DOI: 10.1096/fj.201903188R
[26] S. Lee, P.E. Phelan, R.A. Taylor, R. Prasher, L. Dai. J. Heat Transfer, **138** (5), 051101 (2016). DOI: 10.1115/1.4032310
[27] N.S.S. Mousavi, K.B. Ramadi, Y.-A. Song, S. Kumar. Commun. Mater., **4** (1), 101 (2023). DOI: 10.1038/s43246-023-00429-5
[28] R.T. Richardson, M.R. Ibbotson, A.C. Thompson, A.K. Wise, J.B. Fallon. Healthc. Technol. Lett., **7** (3), 58 (2020). DOI: 10.1049/htl.2019.0114
[29] N. Sarfraz, I. Khan. Chem. Asian J., **16** (7), 720 (2021). DOI: 10.1002/asia.202001202
[30] J. Silver, J.H. Miller. Nat. Rev. Neurosci., **5** (2), 146 (2004). DOI: 10.1038/nrn1326
[31] A. Ranella, M. Barberoglou, S. Bakogianni, C. Fotakis, E. Stratakis. Acta Biomater., **6** (7), 2711 (2010). DOI: 10.1016/j.actbio.2010.01.016
[32] S. Cai, C. Wu, W. Yang, W. Liang, H. Yu, L. Liu. Nanotechnol. Rev., **9** (1), 971 (2020). DOI: 10.1515/ntrev-2020-0076
[33] J. Nurković, I. Zaletel, S. Nurković, Š. Hajrović, F. Mustafić, J. Isma, A. Jurišić Škevin, V. Grbović, M. Kovačević Filipović, Z. Dolićanin. Lasers Med. Sci., **32**, 151 (2017). DOI: 10.1007/s10103-016-2097-2
[34] J. Li, J. Liu, C. Chen. ACS Nano, **11** (3), 2403 (2017). DOI: 10.1021/acsnano.7b01200
[35] P. Bazard, R.D. Frisina, J.P. Walton, V.R. Bhethanabotla. Sci. Rep., **7**, 7803 (2017). DOI: 10.1038/s41598-017-08141-4
[36] M. Kim, J.-H. Lee, J.-M. Nam. Adv. Sci., **6**, 1900471 (2019). DOI: 10.1002/advs.201900471
[37] M. Tian, Y. Ma, W. Lin. Acc. Chem. Res., **52** (8), 2147 (2019). DOI: 10.1021/acs.accounts.9b00289

Translated by T.Zorina